Vol 14 No 11, November 2005
1009-1963/2005/14(11)/2287-07

Chinese Physics

© 2005 Chin. Phys. Soc.
and IOP Publishing Ltd

First principles study on the charge density and the bulk modulus of the transition metals and their carbides and nitrides*

Li Cheng-Bin(李承斌)[a)†], Li Ming-Kai(黎明锴)[a)b)], Yin Dong(尹 东)[c)], Liu Fu-Qing(刘福庆)[a)], and Fan Xiang-Jun(范湘军)[a)‡]

[a)] *Department of Physics and Center of Nanoscience and Nanotechnology Research, Wuhan University, Wuhan 430072, China*

[b)] *Quantum-Functional Semiconductor Research Center, Dongguk University, Seoul 100-715, Korea*

[c)] *Department of Physics, Jianghan University, Wuhan 430056, China*

(Received 6 February 2005; revised manuscript received 11 April 2005)

A first principles study of the electronic properties and bulk modulus (B_0) of the fcc and bcc transition metals, transition metal carbides and nitrides is presented. The calculations were performed by plane-wave pseudopotential method in the framework of the density functional theory with local density approximation. The density of states and the valence charge densities of these solids are plotted. The results show that B_0 does not vary monotonically when the number of the valence d electrons increases. B_0 reaches a maximum and then decreases for each of the four sorts of solids. It is related to the occupation of the bonding and anti-bonding states in the solid. The value of the valence charge density at the midpoint between the two nearest metal atoms tends to be proportional to B_0.

Keywords: density functional theory, plane-wave pseudopotential method, bulk modulus, charge density

PACC: 6220, 7115A, 7115M

1. Introduction

Transition metals (TM) and their carbides (TMC) and nitrides (TMN) usually have good properties of large hardness, high melting point and good wear resistance.[1] They are widely used for hard coating and cutting tools. Many theoretical works have been devoted to the investigation of their electronic structure and bonding characteristics.[2−17] Sigalas and co-workers[3] calculated the total energies, bulk moduli (B_0), equilibrium lattice parameters and band structures for 3d, 4d, and 5d TM by augmented-plane-wave method and presented a study on the crystal structure stability between fcc and bcc structures. Häglund and co-workers[5−8] made systematic investigation on the enthalpy of formation and cohesive properties of TMC and TMN by linear-muffin-tin-orbitals method. Grossman *et al*[9] investigated the trends in electronic and structural properties of TM and their carbides and nitrides, their results showed both increasing the number of d electrons and the presence of f electrons in the core lead larger B_0. Šimůnek and Vackář[15] found a correlation in a form of monotonous dependence between binding energies of core electrons of the constituent atoms and B_0 of TMC and TMN. Assuming that the s-state electrons do not contribute significantly to B_0, Gilman[16] found that, for the TM, the log–log plots of the effective d-electron densities and their corresponding B_0 are linear except for the magnetic elements. For hard metals (such as TiC), B_0 are higher than those of the corresponding pure metals. Gilman thought that these increases are related to the increased density of valence electrons.

In this paper, eight TM elements (from Sc to Ni) are involved. The TM in the fcc and bcc structures and their carbides and nitrides in the NaCl structure are taken into account. We make first principles calculations based on density-function theory (DFT)[18,19]

*Project supported by the National Natural Science Foundation of China (Grant Nos 50175082 and 10275049), and the Fund for the Doctoral Program of Higher Education (Grant No 2002486016).

†E-mail: cbli_whu@163.com

‡Corresponding author. E-mail: xjfan@whu.edu.cn

to the structural and electronic properties of these solids. Our results of the equilibrium lattice constants and B_0 nearly agree with those of the other works. We focus on the correlation of the valence charge density and B_0 and find that B_0 and the valence charge density at the centre of metal–metal bonds tend to be proportional.

2. Method of calculation

For all the TMC and TMN in the NaCl structure appearing in this paper, the metal atom is located at the origin of the unit cell and the non-metal atom is placed at (1/2, 1/2, 1/2). We assume that all the TM in this paper are in nonmagnetic states. The spin-polarization is excluded in the calculations in order to eliminate additional variables to let us focus on the simplest correlation between valence charge density and B_0.

The plane-wave pseudopotential total-energy scheme is used in the current work. The non-semicore Hartwigsen–Geodecker–Hutter (HGH) relativistic separable dual-space Gaussian pseudopotentials[20] in the context of local-density approximation (LDA) are adopted in the calculations. Our calculations are performed by using the ABINIT package[21] in version 4.2.3. The convergency studies related to the plane-wave energy cut-offs and the sampling of the Brillouin zone are carried out in order to choose the proper parameters for the calculations to keep the total energy errors within 10^{-5} Hartree. The $16\times16\times16$ Monkhorst–Pack[22] $\boldsymbol{k}$-point sampling grid is used for all the TM, the $8\times8\times8$ grid is used for the TMC and TMN. The plane-wave cutoffs varies vary from 80 Hartree for Sc in bcc structure to 105 Hartree for NiN. For each solid, the optimal lattice constant $a_{\rm opt}$ of the cubic cell is obtained by an algorithm of optimization at first. Then, 21 sets of DFT calculations are performed by varying the lattice parameter with a step of 0.1 Bohr around $a_{\rm opt}$ for each solid. Fitting these 21 sets of data with the Vinet equation of state (EOS),[23] the theoretical equilibrium lattice constant a_0 and B_0 are obtained. The P–V relation of the Vinet EOS is

$$\begin{aligned} P &= -\,\mathrm{d}E(V)/\mathrm{d}V \\ &= [3B_0(1-x)/x^2]\exp\left[\frac{3}{2}(B_0'-1)(1-x)\right], \quad (1) \end{aligned}$$

noting that $x=(V/V_0)^{1/3}$. Where V_0 is the unit cell volume at zero pressure, $B_0'=\partial B/\partial P$ at zero pressure. At last, a self-consistent calculation with lattice constant a_0 is made to generate the valence charge density and density of state (DOS) of the ground states.

3. Results and discussion

The calculated lattice constants and B_0 of the TM and their carbides and nitrides are shown in Table 1. Our calculated lattice constants and B_0 are respectively underestimated and overestimated, but closed to those of the other theoretical works. We note from Table 1 that, along the row of periodic table, B_0 does not vary monotonously with the increase of the number of valence d electrons. As the number of valence d electrons in the TM atom increases, B_0 increases and reaches a maximum at fcc-Fe, bcc-Mn, FeC and MnN in each of four sorts of solids respectively. Then B_0 decreases as more d electrons add to the metal atom. This variation of B_0 with the number of d electrons indicates the occupation of the bonding and anti-bonding states in the solids.

The DOS of the TM and their carbides and nitrides are shown in Fig.1. Figures 1(a), 1(b), 1(c) and 1(d) are the DOS of the fcc TM, bcc TM, TMC and TMN respectively. The vertical lines in the figures denote the Fermi energy levels. There is no a priori reason for the existence of a clean separation of electronic energy spectrum into bonding, anti-bonding and non-bonding region. But it is often connected with a well-defined minimum in the DOS.[8] The arrows in Fig.1 point to the valleys, which indicate the transition from bonding to anti-bonding states. For the four sorts of solids considered in this paper, the bonding states will be occupied firstly when the number of the valence d electrons in the metal atom increases. The more valence d electrons, the more bonding states will be occupied. It causes increase of B_0. When the bonding states reach the saturation, B_0 reaches the maximum. In this case, the Fermi energy level of the solid which has the largest B_0 usually locates in a valley which indicates the transition from the bonding and anti-bonding states. We can see from Fig.1 that the Fermi levels of fcc-Fe, bcc-Mn, FeC and MnN are located in the valleys that the arrows point to and indicate the transformation from bonding and anti-bonding states. When more valence d electrons are added to the metal atom, they will occupy the anti-bonding states. The anti-bonding states will weaken the strength of the solid and then B_0 decreases.

Table 1. The calculated lattice constants a_0 (nm) and B_0 (GPa) for the transition metals (fcc and bcc structures) and their carbides and nitrides.[24−33] (a_0 and B_0 denote the results of our calculations; $a_{0,\text{others}}$ and $B_{0,\text{others}}$ denotes the other theoretical results.

	a_0/nm	$a_{0,\text{others}}$/nm	$a_{0,\text{expt}}$/nm	B_0	$B_{0,\text{others}}$	$B_{0,\text{expt}}$
Sc_{fcc}	0.445	0.447[3], 0.452[8]		53	54.1[3]	
Ti_{fcc}	0.399	0.400[3], 0.406[8]		112	126[3]	
V_{fcc}	0.372	0.374[3], 0.379[8]		195	208[3]	
Cr_{fcc}	0.353	0.356[3], 0.360[8]	0.368[26]	258	265[3]	
Mn_{fcc}	0.343	0.344[3], 0.349[8]	0.386[26]	326	335[3]	
Fe_{fcc}	0.338	0.339[3], 0.338[25]	0.365[26]	338	339[3], 344[25]	
Co_{fcc}	0.338	0.339[3], 0.342[8]	0.354[26]	306	249[3]	191[33]
Ni_{fcc}	0.343	0.343[3], 0.345[8]	0.352[26]	261	274[3]	186[33]
Sc_{bcc}	0.355	0.357[3]		55	59.7[3]	
Ti_{bcc}	0.315	0.317[3]	0.307[26]	111	125[3], 120[4]	
V_{bcc}	0.292	0.293[3]	0.303[26]	200	223[3], 200[4]	162[33]
Cr_{bcc}	0.278	0.280[3]	0.288[26]	289	305[3], 280[4]	190[33]
Mn_{bcc}	0.273	0.274[3]	0.308[26]	324	322[3]	
Fe_{bcc}	0.270	0.271[3], 0.270[25]	0.287[26]	322	311[3], 314[25]	
Co_{bcc}	0.270	0.269[3], 0.274[24]	0.282[27]	297	354[3]	
Ni_{bcc}	0.272	0.273[3]		258	234[3]	
ScC	0.454			157		
TiC	0.423	0.438[9]	0.431[30]	263	267[9]	240[30]
VC	0.407	0.422[9]		332	321[9]	
CrC	0.399	0.410[9]		362	351[9]	
MnC	0.395			376		
FeC	0.392			380		
CoC	0.393			359		
NiC	0.399			311		
ScN	0.437	0.445[25]	0.450[28]	202		182±40[28]
TiN	0.415	0.432[9]	0.424[29]	296	304[9]	320[31]
VN	0.405	0.419[9]	0.414[29]	330	338[9]	
CrN	0.398	0.409[9]	0.416[32]	368	361[9]	
MnN	0.395			373		
FeN	0.393			368		
CoN	0.393			362		
NiN	0.399			309		

It can be also noted from Table 1 that, for the same element, B_0 of TMC and TMN are larger than those of the pure metals. It should be caused by the presence of C and N. There are only metal–metal bonds in the pure metals. But except metal–metal bonds, the presence of nonmetal atoms (C and N) introduces a different kind of bonding between metal and nonmetal atoms. Figure 2 shows us the partial DOS of FeC and MnN. Figure 2(a) is the DOS of FeC and Fig.2(b) is the DOS of MnN. It can be noted from Fig.2 that there are hybridized nonmetal p-metal d states between metal and nonmetal atoms. These hybridized p-d states mainly locate in the bonding region and cause B_0 of TMC and TMN larger than the corresponding pure metals.

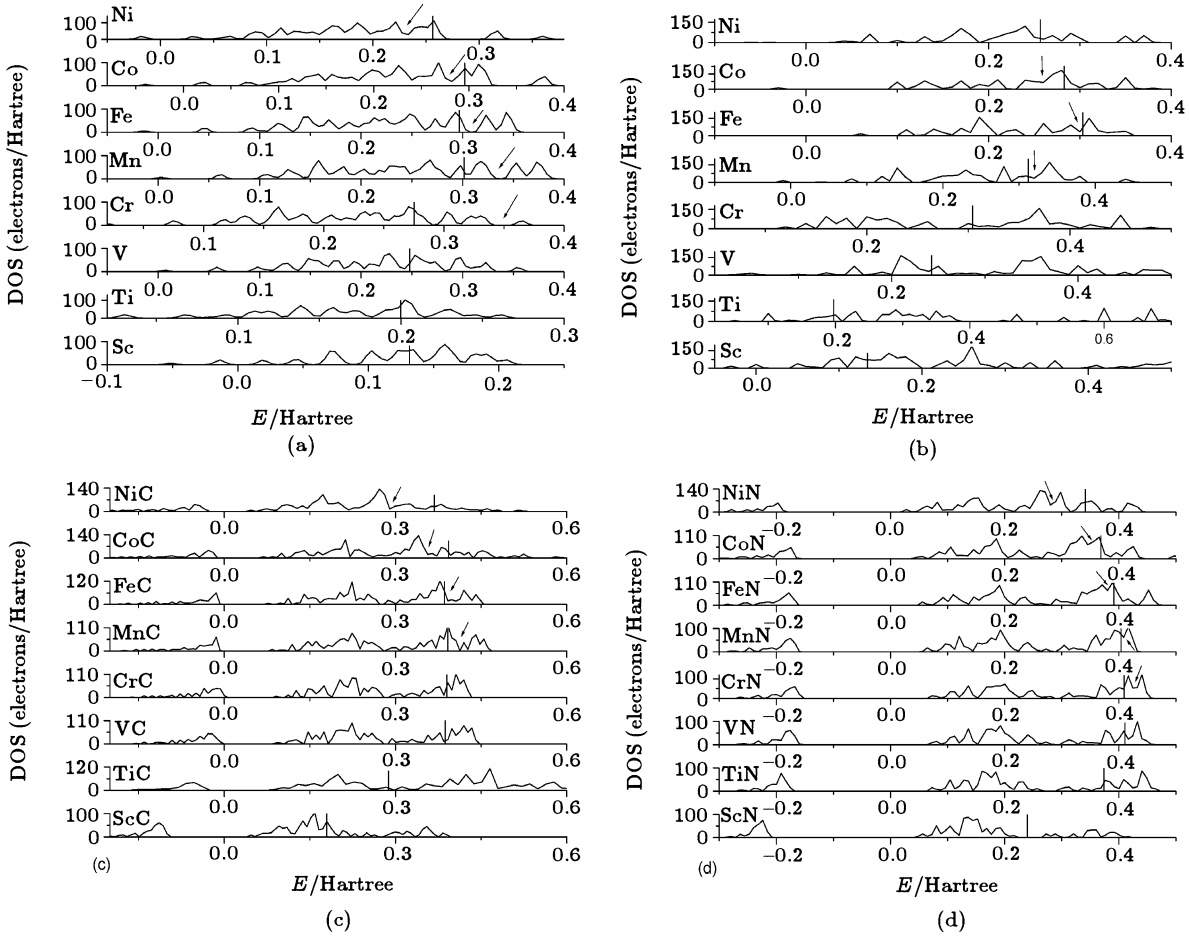


Fig.1. The DOS of transition metals and their carbides and nitrides. (a) for fcc transition metals, (b) for bcc transition metals, (c) for transition metal carbides and (d) for transition metal nitrides. The vertical lines in the figures denote the Fermi energy levels. The arrows in the figures point to the valleys and indicate the transition from bonding to anti-bonding states. Note: 1Hartree=2Rydberg=27.2eV.

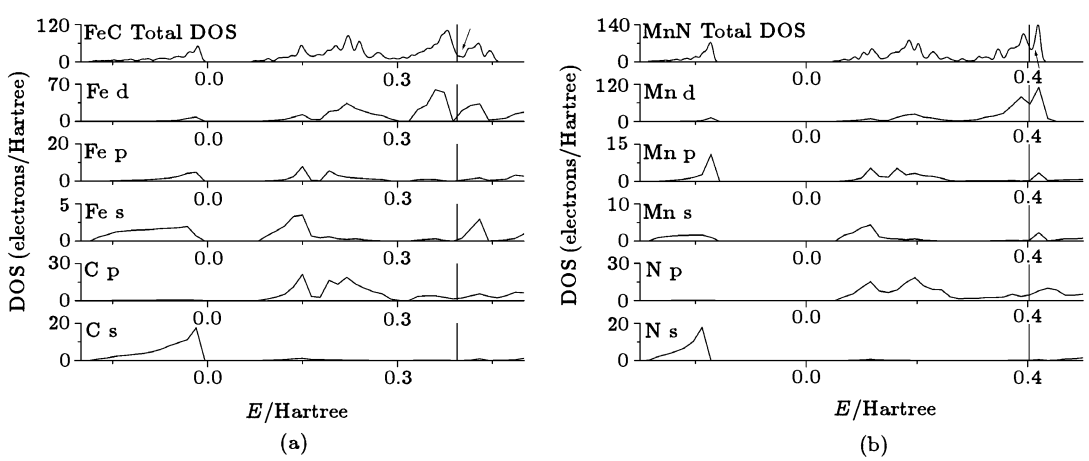


Fig.2. The partial DOS of Fec and MnN. (a) is for the FeC and (b) is for MnN. The vertical lines denote the Fermi energy levels. The arrows in the figures point to the valleys and indicate the transition from bonding to anti-bonding states.

The valence charge densities of TM and their carbides and nitrides are also calculated. The valence charge density distributions between the two nearest metal atoms in the solids are shown in Fig.3. Figure 3(a) is for the fcc TM, 3(b) for the bcc TM, 3(c) for TMC and 3(d) for TMN. All the distances be-

tween the two nearest metal atoms are normalized to 1 in Fig.3. It can be noted that the value of the valence charge density at the centre of the metal–metal bonding (ρ_{mid}) increases from the beginning when the number of valence d electrons increases. And this value will reach the maximum and then decrease when the number of valence d electrons keeps on increasing. This trend is almost the same as the trend of B_0.

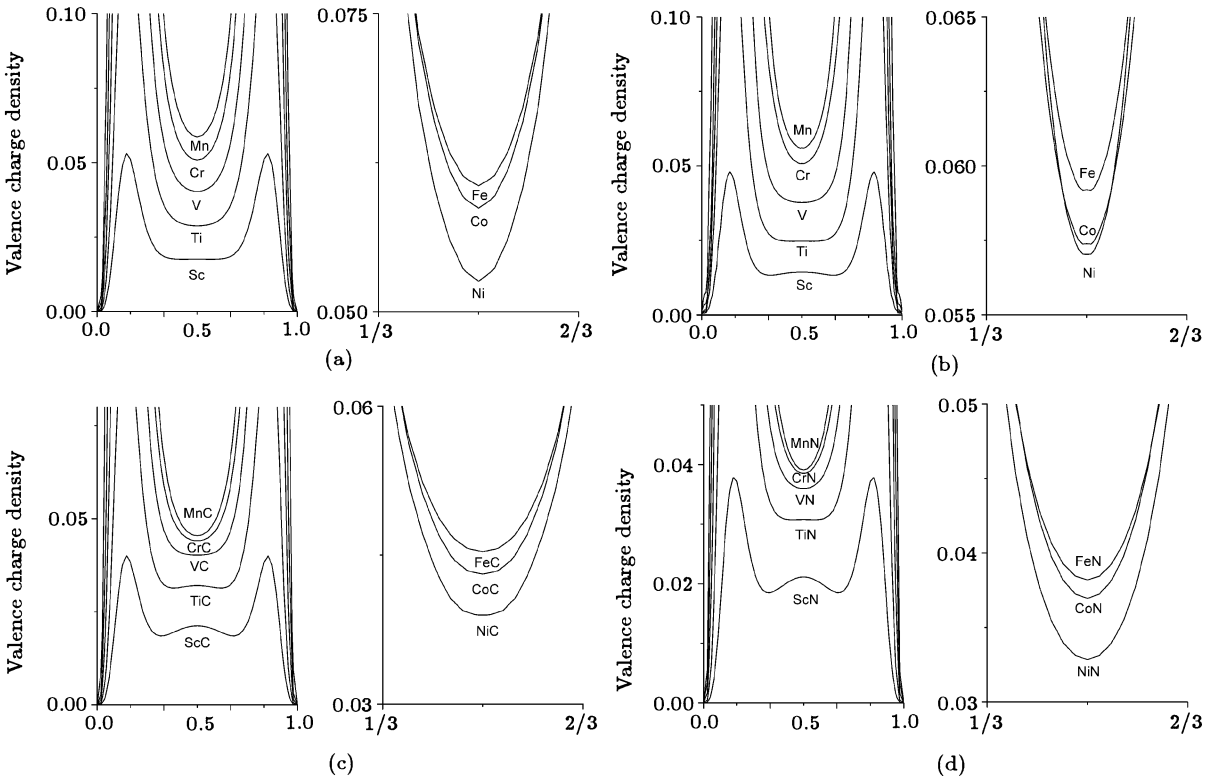


Fig.3. The valence charge density distribution between the two nearest metal atoms. (a) for fcc transition metals, along [110] direction; (b) for bcc transition metals, along [111] direction; (c) for transition metal carbides, along [110] direction; and (d) for transition metal nitrides, along [110] direction. The x axis corresponds to the distance between the two nearest metal atoms and all these distances are normalized to 1. The y axis corresponds to the valence charge density, in unit electrons/Bohr^3.

The correlation between B_0 and the charge density is shown in Fig.4. The plots of B_0 and ρ_{mid} for the four sorts of solids are linear with high correlation coefficients. For the first four metals, bcc TM have larger B_0 than fcc TM except that B_0 of bcc and fcc Ti are almost the same. And then the trend reverses. There are only metal–metal bonds in the fcc and bcc TM. The higher ρ_{mid} indicates the more bonding states and the less anti-bonding states are occupied. The value of ρ_{mid} reflects the strength of the metal–metal bonds. ρ_{mid} of the later four fcc metals are higher than those of the bcc metals, and so they are stiffer than the corresponding bcc metals. ρ_{mid} of the bcc V and Cr are higher than the fcc V and Cr respectively, and as a result B_0 are larger than the fcc V and Cr. ρ_{mid} of the bcc and fcc Ti are nearly the same and ρ_{mid} of the bcc Ti is a bit lower than the fcc Ti. And this tiny difference still affects B_0 of Ti. B_0 of bcc Ti is 111GPa and B_0 of fcc Ti is 112GPa. Sc is an exception that fcc structure has higher ρ_{mid} but with lower B_0. It should be given further consideration.

There are two types of bonds in the TMC and TMN—metal-nonmetal bonds and metal–metal bonds. The additional metal–nonmetal bonds lead B_0 of the TMC and TMN larger than the corresponding pure metals. And because of the electronegativities of C and N, more electrons are attracted around nonmetal atoms and ρ_{mid} of the TMC and TMN are lower than those of the corresponding pure metals. Since the electronegativity of N is larger than C, then its ability of attracting electrons is higher than C and as a result ρ_{mid} of TMN is lower than TMC for the same metal element.

The metal-nonmetal bonds in TMC and TMN are dominated by the hybridized p–d states. The metal d states have small overlap with the nonmetal p states and contribute more to the metal–metal bonds.[8] For

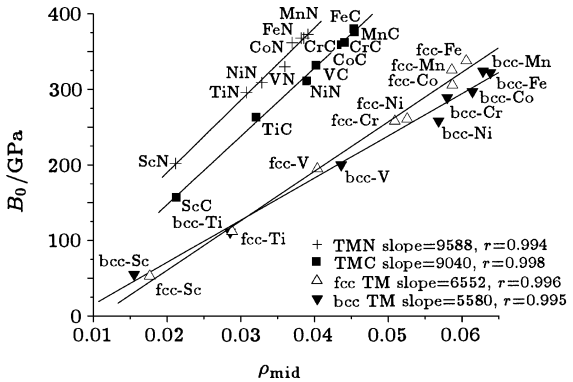


Fig.4. The correlation between the bulk modulus (B_0) and valence charge density. $\rho_{\rm mid}$ is the valence charge density at the midpoint between the two nearest metal atoms, in unit electrons/Bohr^3. $\rho_{\rm mid}$ and B_0 tend to be proportional. r is the correlation coefficient.

each of the four sorts of solids in this paper, the occupation of the bonding and anti-bonding states is related to $\rho_{\rm mid}$. When the number of the valence d electrons increases from the beginning, the bonding states are occupied firstly. The more bonding states are occupied, the more valence charges are accumulated at the centre of the metal–metal bonds. So $\rho_{\rm mid}$ and B_0 increase. When the bonding states are saturated, $\rho_{\rm mid}$ and B_0 reach their maximums. The occupation of the anti-bonding states will cause decrease of $\rho_{\rm mid}$ and the bulk modulus. It can be noted obviously from Fig.4 that the bulk modulus and $\rho_{\rm mid}$ tend to be proportional. We can choose $\rho_{\rm mid}$ as the parameter to scale the strength of the solids in which there are metal–metal bonds.

4. Summary

A series of first principles calculations for the electronic properties and B_0 of the fcc and bcc TM and their carbides and nitrides have been carried out. The variation of B_0 of these four sorts of solids with the number of valence d electrons is related to the occupation of the bonding and anti-bonding states. The more valence d electrons, the more bonding states are occupied and the larger B_0 is for each of the four sorts of solids. B_0 reaches the maximum when the bonding states are saturated. The anti-bonding states will be occupied when the number of the valence d electrons keeps on increasing. B_0 will decrease as a result. The valence charge density at the centre of the metal–metal bonds tends to be proportional to B_0 for each of the four sorts of solids.

References

[1] Holleck H 1986 *J. Vac. Sci. Technol.* A **4** 2661
[2] Neckel A, Rastl P, Eibler R, Weinberger P and Schwarz K 1976 *J. Phys.* C *Solid State Phys.* **9** 579
[3] Sigalas M, Papaconstantopoulos D A and Bacalis N C 1992 *Phys. Rev.* B **45** 5777
[4] Paxton A T, Methfessel M and Polatoglou H M 1990 *Phys. Rev.* B **41** 8127
[5] Häglund J, Grimvall G, Jarlborg T and Fernández Guillermet A 1991 *Phys. Rev.* B **43** 14400
[6] Fernández Guillermet A, Häglund J and Grimvall G 1992 *Phys. Rev.* B **45** 11557
[7] Fernández Guillermet A, Häglund J and Grimvall G 1993 *Phys. Rev.* B **48** 11673
[8] Häglund J, Fernández Guillermet A and Grimvall G 1993 *Phys. Rev.* B **48** 11685
[9] Grossman J C, Mizel A, Côté M, Cohen M L and Louie S G 1999 *Phys. Rev.* B **60** 6343
[10] Jhi S H, Louie S G, Cohen M L and Ihm J 2001 *Phys. Rev. Lett.* **86** 3348
[11] Jhi S H and Ihm J 1997 *Phys. Rev.* B **56** 13826
[12] Jhi S H, Ihm J, Louie S G and Cohen M L 1999 *Nature* **399** 132
[13] Song Y, Yang R, Li D, Wu W T and Guo Z X 1999 *Phys. Rev.* B **59** 14220
[14] Cheng D, Wang S and Ye H 2001 *Phys. Rev.* B **64** 024107
[15] Šimůnek A and Vackář J 2001 *Phys. Rev.* B **64** 235115
[16] Gilman J J 2003 *Electronic Basis of the Strength of Materials* (Cambridge: Cambridge University Press) p117
[17] Hua J S, Jing F Q, Dong Y B, Tan H, Shen Z Y, Zhou X M and Hu S L 2003 *Acta Phys. Sin.* **52** 2005 (in Chinese)
[18] Hohenberg P and Kohn W 1964 *Phys. Rev.* **136** B864
[19] Kohn W and Sham L J 1965 *Phys. Rev.* **140** A1133
[20] Hartwigsen C, Geodecker S and Hutter J 1998 *Phys. Rev.* B **58** 3641
[21] The ABINIT code is a common project of the Universite Catholique de Louvain, Corning Incorporated and other contributors. (URL http://www.abinit.org)
[22] Monkhorst H J and Pack J D 1976 *Phys. Rev.* B **13** 5188
[23] Vinet P, Rose J H, Ferrante J and Smith J R 1989 *J. Phys. Condens. Matter* **1** 1941
[24] Liu A Y and Singh D J 1993 *Phys. Rev.* B **47** 8515
[25] Wang C S, Klein B M and Krakauer H 1985 *Phys. Rev. Lett.* **16** 1852
[26] Barrett C S and Massalski T B 1980 *Structure of Metals* 3rd ed. (Oxford: Pergamon Press) p626
[27] Idzerda Y U, Elam W T, Jonker B T and Prinz G A 1989 *Phys. Rev. Lett.* **62** 2480
[28] Gall D, Petrov I, Hellgren N, Hultman L, Sundgren J E and Greene J E 1998 *J. Appl. Phys.* **84** 6034
[29] Barnett S A and Shinn M 1994 *Annu. Rev. Mater. Sci.* **24** 481
[30] Pintschovius L, Reichardtm W and Scheerer B 1978 *J. Phys.* C *Solid State Phys.* **11** 1557
[31] Spengler W, Kaiser R, Christensen A N and Müller-Vogt G 1978 *Phys. Rev.* B **17** 1095
[32] Almer J, Lienert U, Peng R L, Schlauer C and Odén M 2003 *J. Appl. Phys.* **94** 697
[33] Kittle C 1976 *Introduction to Solid State Physics* 5th ed (New York: Wiley) p56